Title: Entropy-Driven Supramolecular Ring-Opening Polymerization of a Cyclic Hemoglobin Monomer for Constructing a Hemoglobin−PEG Alternating Polymer with Structural Regularity

Authors:

*Takashi Matsuhira, Hiromi Sakai**

Affiliation:

Department of Chemistry, Nara Medical University, 840 Shijo-cho, Kashihara, 634-8521 Japan

*Corresponding Author:

Hiromi SAKAI, Ph.D. (D.Eng.), Ph.D. (D. Med.Sci.)

Professor of Chemistry

Nara Medical University

840 Shijo-cho, Kashihara, Nara 634-8521, Japan

Tel/Fax: +81-744-29-8810

E-mail: hirosakai@naramed-u.ac.jp

Abstract

Our earlier report described that a cyclic hemoglobin (Hb) monomer with two β subunits of an Hb molecule ($\alpha_2\beta_2$) bound through a flexible polyethylene glycol (PEG) chain undergoes reversible supramolecular ring-opening polymerization (S-ROP) to produce a supramolecular Hb polymer with an Hb−PEG alternating structure. In this work, we polymerized cyclic Hb monomers with different ring sizes (2, 5, 10, or 20 kDa PEG) to evaluate the thermodynamics of S-ROP equilibrium. Quantification of the produced supramolecular Hb polymers and the remaining cyclic Hb monomers in the equilibrium state revealed a negligibly small enthalpy change in S-ROP ($\Delta H_p \leq 1$ kJ·mol^{-1}) and a markedly positive entropy change increasing with ring size (ΔS_p = 26.8−33.2 J·mol^{-1}·K^{-1}). Results suggest an entropy-driven mechanism in S-ROP: a cyclic Hb monomer with the larger ring size prefers to form a supramolecular Hb polymer. S-ROP used for this study has potential to construct submicrometer-sized Hb−PEG alternating polymers having structural regularity.

Keywords

blood substitutes, cross-linking, hemoglobin-based oxygen carriers, PEGylation, polymerized protein, supramolecular chemistry

1. Introduction

Hemoglobin (Hb), the most abundant protein in mammalian blood, plays an important role in oxygen transport. During the last half century, many attempts have been made to create artificial oxygen carriers through the modification of isolated Hb molecules for use as red blood cell (RBC) substitutes.[1] Such Hb-based oxygen carriers (HBOCs) are expected to overcome existing transfusion-related problems such as pathogen contamination, blood type mismatching, and short shelf life.[1] However, free Hb molecules in plasma cause severe renal and cardiovascular toxicities when injected into blood circulation.[2] To reduce toxicities, cellular and acellular types of HBOCs have been developed. Cellular HBOCs have been produced by encapsulation of Hbs with synthetic polymer membranes or in phospholipid vesicles (liposomes) mimicking the cellular structure of RBCs.[1,3,4] Acellular HBOCs have been produced by various chemical modification of Hbs. For instance, intra-molecular αα-cross-linking or ββ-cross-linking inhibits dissociation of an $\alpha_2\beta_2$ tetrameric Hb molecule.[5,6] Conjugations of polyethylene glycols (PEG) or albumins lower the antigenicity of an Hb molecule by surface coating.[7–9] Moreover, inter-molecular conjugation of multiple Hbs by glutaraldehyde enlarges the particle.[10]

Despite pioneers' efforts, it remains difficult to block the Hb toxicity completely by chemical modification. In fact, severe cardiovascular adverse effects were found during clinical trials of polymerized Hbs (poly-Hb) obtained by cross-linking with glutaraldehyde.[11] Reportedly, adverse effects of poly-Hb were caused mainly by the presence of a minor component with molecular weight below 256 kDa.[12] Smaller molecules tend to flow near the vessel wall. Furthermore, such a low molecular weight component of poly-Hb, which has a sufficiently small particle size for extravasation, is expected to scavenge an endogenous vasorelaxant, nitric oxide (NO), causing vasoconstriction and hypertension.[13] Therefore, development of highly efficient

polymerization for Hbs is now regarded as a promising strategy for reducing the cardiovascular toxicity of HBOCs.

Several methods have been developed for synthesizing submicrometer or micrometer sized poly-Hb. Hb-microparticles have been fabricated by polymerizing Hb in the porous $CaCO_3$ microparticles used as a temporary template.[14] Also, Hb-albumin microspheres have been produced by polymerization in a water/oil (w/o) emulsion formed via a porous glass membrane.[15] Submicrometer Hb particles (250 nm) have been synthesized using precipitation polymerization.[16] Furthermore, cross-linking agents of various kinds have been developed to replace glutaraldehyde in production of polymerized Hbs with different structures: multi-functional PEGs,[17] oligosaccharide,[18] polysaccharide,[3] polyamide linker,[19] and carbodiimede.[20] Additionally, we recently reported the efficient synthesis of Hb−PEG alternatively aligned linear polymer by ring-opening polymerization (ROP) based on supramolecular chemistry.[21]

Supramolecular chemistry, a rapidly growing area, treats assemblies consisting of discrete molecular subunits bound through non-covalent interactions.[22] Interactions are reversible and weak compared to those of covalent bonding. For that reason, supramolecular materials realize unique structures, functions, and properties. An Hb molecule is also categorized as a supramolecular assembly that consists of two α and two β subunits ($\alpha_2\beta_2$). They are assembled using a combination of non-covalent interactions as hydrogen bonds, hydrophobic forces, van der Waals forces, and electrostatic effects. The $\alpha_2\beta_2$ tetramer dissociates reversibly into dimers ($\alpha_2\beta_2 \rightleftarrows 2\alpha\beta$), and thereby inter-molecularly exchanges αβ dimers,[6] although it favors fundamentally stable $\alpha_2\beta_2$ tetrameric structure under physiological conditions.[23]

Reportedly, supramolecular protein polymers are induced via specific interactions of proteins such as heme–heme pocket interaction,[24] coiled−coil interaction,[25] helix bundle folding,[26] hapten–antibody complex formation,[27] and inter-subunit interaction.[28] Our aim is to construct a supramolecular polymer via reversible interactions between αβ subunits of Hb as a precursor of the covalently fixed Hb−PEG alternating polymer.

In our earlier study, a bi-functional 10 kDa maleimide-PEG (mal_2-PEG) was reacted with two Cys-93(β) of an Hb unit ($\alpha_2\beta_2$) to obtain a cyclic Hb monomer CM-10 (**Figure 1A**).[21] During the inter-monomer subunit exchange of αβ dimers, CM-10 induced supramolecular ring-opening polymerization (S-ROP) to form a supramolecular Hb polymer (SP-10, **Figure 1B**). The SP-10 consists of monomer units that are bound reversibly through the non-covalent inter-subunit interactions of αβ dimers at the PEG terminals. The Hb units ($\alpha_2\beta_2$) in the constructed SP-10 and remaining CM-10 were subsequently fixed covalently by reaction with bis-(3,5-dibromosalicyl) fumarate (DBBF) to obtain ββ-cross-linked products (XLSP-10 and XLCM-10). In this reaction, DBBF is known to be a site-specific ββ-cross-linker that binds two Lys-82(β) residues through fumarate.[29] Quantification of the stable ββ-cross-linked products using size exclusion chromatography (SEC) has made it possible to analyze the ratio of SP-10 (polymer) and CM-10 (monomer) in the equilibrium state of S-ROP immediately before reaction with DBBF. That quantification revealed that CM-10 assembled to form SP-10 at a higher concentration, and that SP-10 dissociated to CM-10 at a lower concentration. However, the mechanism of S-ROP has not been clarified completely. Moreover, the effect of PEG length should be evaluated to optimize the polymerization efficiency.

In the present work, cyclic Hb monomers using 2, 5, 10, or 20 kDa PEG linkers (CM-2, -5, 10, and -20 in **Figure 1B**) were synthesized to evaluate the ring size effects. By applying the

procedures described in the earlier report,[21] the constructed Hb−PEG alternating supramolecular polymers (SP-2, -5, 10, and -20) and remaining CMs were fixed covalently and were then analyzed using SEC, electrophoresis (SDS-PAGE), and dynamic light scattering (DLS) to compare the polymerization efficiency. Furthermore, for evaluation of the mechanisms, each S-ROP equilibrium was analyzed based on the quantification of ββ-cross-linked products using SEC. We applied thermodynamic analysis commonly used for non-supramolecular ROP of low molecular weight cyclic monomers, such as lactones,[30] toward S-ROP of the giant monomers, CMs. The obtained thermodynamic parameters clarified that S-ROP of all the CMs proceeded with an entropy-driven mechanism.

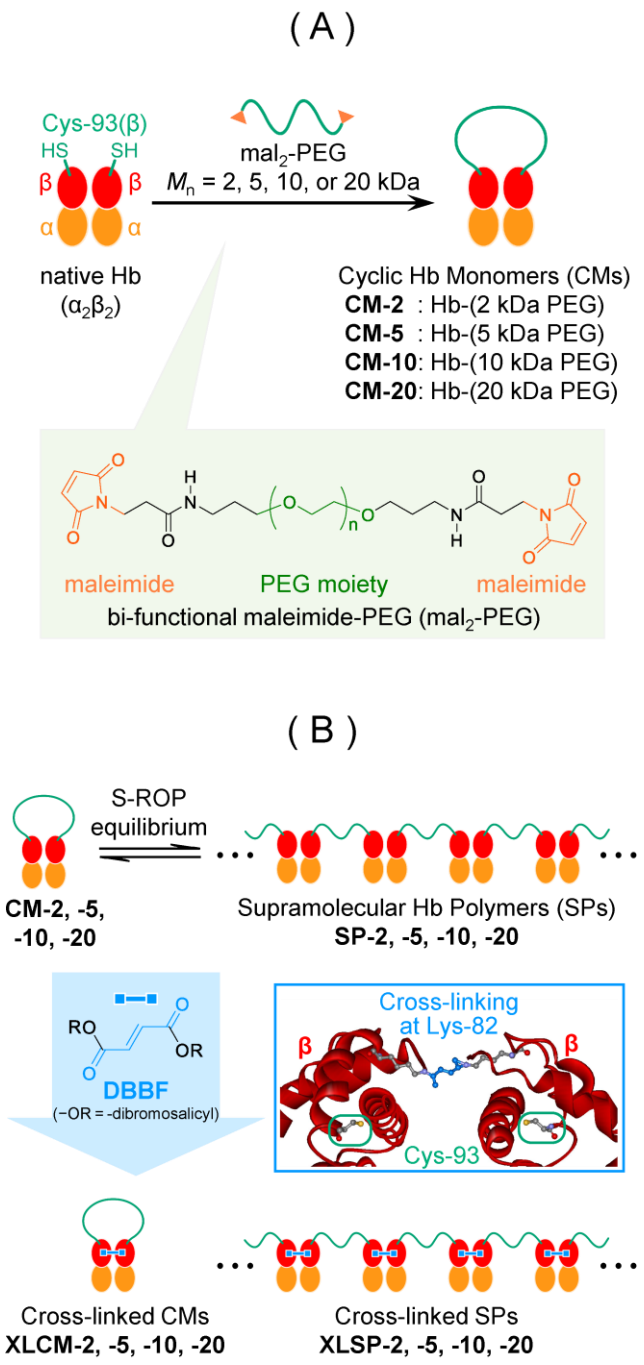

Figure 1. (A) Synthesis of four cyclic Hb monomers (CM-2, -5, -10, and -20), of which two Cys-93 (β) thiols were bridged via 2, 5, 10, and 20 kDa bi-functional maleimide-PEG (mal_2-PEG). (B) Supramolecular ring-opening polymerization (S-ROP) equilibrium between CMs and SPs, and subsequent covalent fixing of Hb units by reaction with bis-(3,5-dibromosalicyl)

fumarate (DBBF). CMs induce S-ROP reversibly by inter-molecular exchange of αβ subunits to produce the corresponding SPs. The equilibrated CMs and SPs are fixed by site-specific cross-linking of two β subunits in each Hb unit ($\alpha_2\beta_2$) by reacting with bis-(3,5-dibromosalicyl) fumarate (DBBF) to produce the corresponding ββ-cross-linked products (XLCMs and XLSPs). The X-ray crystal structure (PDB ID: 1BIJ) of the ββ-cross-linked Hb (XLHb) is shown, particularly presenting the binding sites for maleimide (Cys-93(β)) and DBBF (Lys-82(β)).[29]

2. Materials and Methods

2.1. General procedures

A highly purified human carbonyl Hb (native Hb) was isolated by pasteurization and nanofiltration from RBCs provided by the Japanese Red Cross.[4] The concentrations of Hb units in modified Hbs were determined using a kit (Hemoglobin B-test Wako; Fujifilm Wako Pure Chemical Corp., Tokyo, Japan) with a UV-vis spectrometer (V-660; JASCO Corp., Tokyo, Japan). Four bi-functional maleimede PEGs (mal_2-PEG) of Mal-PEG-Mal-2k (Batch No. 20180920BL03, molecular weight 2 kDa, purity 95%; Biochempeg Scientific Inc., Massachusetts, U.S.A.), MAL-PEG-MAL-5000 (Lot No. 152-118, M_n 4,400, purity 98%; Laysan Bio Inc., Alabama, U.S.A.), SUNBRIGHT DE-100MA (Lot M153536, M_n 10456, M_w/M_n = 1.02, substitution 90.6%; NOF Corp., Tokyo, Japan), and SUNBRIGHT DE-200MA, Lot M179584, M_n 20815, M_w/M_n = 1.03, substitution 92.6%; NOF Corp.) were used respectively, for the syntheses of four cyclic Hb monomers. In addition, bis-(3,5-dibromosalicyl) fumarate (DBBF; Abcam plc., Cambridge, U.K.) was used for intra-molecular ββ-cross-linking of Hb units.

2.2. Synthesis of cyclic Hb monomers (CMs)

The cyclic Hb monomers (CM-2, CM-5, CM-10, and CM-20) were obtained according to methods reported earlier[21,31] by reacting four mal_2-PEGs with native Hb (**Figure 1A**). Mal_2-PEG was excessive in the synthesis of CM-2.[31] Also, Hb was excessive in that of CM-5, -10, and -20.[21] Powdered 2 kDa mal_2-PEG (201.7 mg, 85.4 μmol) was added to 27.54 mL of 1.55 mM (10.0 g/dL) native Hb solution (42.7 μmol, 0.50 eq.[31]) in phosphate buffered saline (PBS, pH 7.4,

137 mM NaCl, 2.7 mM KCl, 10 mM Na_2HPO_4, and 1.8 mM KH_2PO_4). Similarly, 5 kDa mal_2-PEG (530 mg, 120 μmol), 10 kDa mal_2-PEG (1.01 g, 96.6 μmol), and 20 kDa mal_2-PEG (2.19 g, 105 μmol) were added, respectively, to 1.2 molar equivalent[21] 10.0 g/dL native Hb solutions in PBS. Each reaction mixture was stirred overnight under a CO atmosphere at 4 °C. The produced CMs were purified by salting out fractionation using ammonium sulfate. Then the remaining excess salts were removed by dialysis. Finally, the CM solutions were concentrated using osmotic pressure difference from concentrated PEG 20,000 solution[21] to obtain 2.43 mL of 5.77 mM CM-2 solution (yield 32.9%), 23.20 mL of 3.16 mM CM-5 solution (yield 50.7%), 23.62 mL of 3.24 mM CM-10 solution (yield 65.0%), and 63.13 mL of 1.16 mM CM-20 solution (yield 58.1%).

2.3. Size exclusion chromatography (SEC)

SEC was conducted using an HPLC system (Chromaster; Hitachi High-Technologies Corp.) equipped with an SEC column (Shodex Protein KW-804; Showa Denko K.K., Tokyo, Japan) at an ambient temperature (20−30 °C). The separation range of this column is 30 to ca. 4,000 kDa for proteins. Effluent was monitored using a diode array detector (5430; Hitachi High-Technologies Corp.) with absorbance at 419 nm, which corresponds to λ_{max} of the Soret band of carbonyl Hb. Each modified Hb solution was diluted with PBS to 0.050 mM and was filtered through a syringe-driven filter unit (Millex 0.22 μm PVDF filter; Merck Millipore Ltd., Merck KGaA, U.S.A. or DISMIC-25CS020AS 0.20 μm cellulose acetate filter; Toyo Roshi Kaisha, Ltd., Tokyo, Japan). Then 20 μL of analyte was injected into the SEC column through a sampler. PBS (pH 7.4) was used as an eluent with a 1.0 mL/min flow rate.

2.4. Sodium dodecyl sulfate polyacrylamide gel electrophoresis (SDS-PAGE)

All solutions of Hb derivatives were diluted with PBS to the Hb concentration of 0.012 mM. Then, each resulting solution was mixed with a half volume of the denaturing buffer[32] (0.19 M Tris-HCl buffer pH 6.8, containing 6.0% (wt/v) sodium dodecyl sulfate (SDS), 15% (v/v) 2-mercaptoethanol, 30% (wt/v) sucrose, and 0.006% (wt/v) bromophenol blue) and incubated at 80 °C for 15 min. Electrophoresis was performed on a 13% polyacrylamide mini-slab gel using a mini-slab electrophoresis system (NA-1010; Nihon Eido Corp., Tokyo, Japan). An Amersham Low Molecular Weight Calibration Kit for SDS Electrophoresis (GE Healthcare Japan Ltd., Tokyo, Japan) was used for molecular weight markers. After the gels were stained with Coomassie brilliant blue (Quick CBB; Fujifilm Wako Pure Chemical Corp.), images of the stained gels were obtained using transmission scanning (GT-F650; Seiko Epson Corp., Nagano, Japan).

2.5. Dynamic light scattering (DLS)

For DLS measurements, CM-2, -5, -10, and -20 were reacted with 2.0 molar equivalent DBBF, respectively at initial monomer concentrations, $[M]_0$, of 5.43, 3.10, 3.01, and 1.16 mM to obtain corresponding XLSP-2, -5, -10, and -20 solutions. The Hb concentrations of CMs and XLSPs were adjusted to 0.010 mM in PBS (pH 7.4); then each solution was filtered through a syringe-driven filter unit (Millex 0.22 μm PVDF filter; Merck Millipore Ltd.) to remove dust. The particle diameter distribution was measured using a nanoparticle size analyzer (SZ-100-S;

Horiba Ltd., Tokyo, Japan) equipped with a 10 mW laser (λ = 532 nm) at 25 °C. The light-scattering signal was detected at 173° (backscatter detection). Correlation data were analyzed using software (NextSpec 1.80; Horiba Ltd.). The particle diameter distribution was obtained using a standard monodispersed model based on the scattering light intensity (rather than number or volume), which emphasized the higher molecular weight components. The particle size distribution histograms of CMs and XLSPs are presented in Supporting Information (**Figure S1**).

2.6. Colloid osmotic pressure (COP)

COP measurements of the CMs were conducted using a colloid osmometer (OSMOMAT 050; Gonotec GmbH, Berlin, Germany) at several protein concentrations at ca. 23 °C. The COP (π) is defined as shown in **Eq. 1** using number-average molecular weights (M_n), the concentration of Hb units (C), the gas constant (R = 62.364 Torr·L·mol^{-1}·K^{-1}), the absolute temperature (T), and the second and the third virial coefficients (A_2, A_3).[33]

$$\pi = RT\left(\frac{C}{M_n} + A_2C^2 + A_3C^3 + \cdots\right) \qquad \cdots (1)$$

Eq. 1 is converted to **Eq. 2**.

$$\frac{\pi}{C} = RT\left(\frac{1}{M_n} + A_2C + A_3C^2 + \cdots\right) \qquad \cdots (2)$$

The plots of π/C versus C for CMs can be fitted to quadratic regression curves by ignoring the higher-order virial coefficient terms of **Eq. 2**. From the intercept $(\pi/C)_{C\to 0}$ of the fitted curve, $1/M_n$ is obtained according to **Eq. 3**.

$$\frac{1}{M_{\mathrm{n}}} = \frac{1}{RT}\left(\frac{\pi}{C}\right)_{C\to 0} \qquad \cdots (3)$$

For comparison, ββ-cross-linked CM-10 (XLCM-10) with a maintained ring-closed structure was synthesized. To a 385 mL PBS solution of CM-10 (0.050 mM, 19.3 μmol) was added 1.6 molar equivalent of powdered DBBF (20.6 mg, 30.8 μmol, 1.6 eq.). It was then stirred overnight under a CO atmosphere at 4 °C. The reaction mixture was filtered. Then it was concentrated by ultrafiltration using a labscale tangential flow filtration system (Merck Millipore Ltd.) equipped with a cassette (Pellicon XL, Biomax 8 kDa, 50 cm^2 filtration area; Merck Millipore Ltd.) to obtain 5.0 mL XLCM-10 solution (1.52 mM, [Hb] = 9.78 g/dL, yield 39.3%). The obtained XLCM-10 was characterized using SEC and SDS-PAGE. Then COP was measured similarly as CMs.

2.7. Quantification of supramolecular ring-chain equilibria by ββ-cross-linking

According to earlier reported methods,[6,21] all Hb units in the equilibrated CMs and SPs were reacted with 2.0 molar equivalent DBBF at 4 °C to produce ββ-cross-linked products (XLCMs and XLSPs) (**Figure 1B**). The cross-linking reactions were conducted respectively at several $[M]_0$ in the ranges of 0.050−5.43 for CM-2, 0.050−3.10 for CM-5, 0.016−3.01 for CM-10, and 0.010−1.16 mM for CM-20.

After reacting CM with DBBF at various concentrations, the product is the mixture of XLCM and XLSP. The relative ratio of XLCM (r_1) is defined as **Eq. 4** using the peak areas of XLCM (S_{XLCM}) and all other areas of XLSP (S_{XLSP}) in the SEC analysis.

$$r_1 = \frac{S_{\mathrm{XLCM}}}{S_{\mathrm{XLCM}} + S_{\mathrm{XLSP}}} \qquad \ldots(4)$$

The r_1 value reflects the ratio of CM in the equilibrium state of S-ROP because the ratio of XLCM is regarded as coinciding with that of corresponding CM immediately before ββ-cross-linking.[21]

2.8. Thermodynamic analysis of S-ROP equilibria

Similarly to section ***2.7***, CMs and SPs in the equilibrium state were ββ-cross-linked at five temperatures (4, 15, 25, 35, and 45 °C) with the unified $[M]_0$ at 1.00 mM. The ββ-cross-linking was monitored by SEC. The ββ-cross-linked products were quantified using SEC to determine the concentration of the remaining CM ($[M]_{eq}$) in the equilibrium state of S-ROP immediately before adding DBBF.

In the case of representative non-supramolecular ROP of low molecular weight cyclic monomers such as cycloalkanes, lactones, lactams, lactides, cyclic (thio)ethers, cyclic phosphates, and cyclosiloxanes, the ratio of monomer conversion depends on the temperature.[34] In the study of ROP for such small molecules, the monomer concentration in an equilibrium state $[M]_{eq}$ can be expressed as a function of the temperature T according to Dainton's equation (**Eq. 5**).[35]

$$\ln[\mathrm{M}]_{\mathrm{eq}} = \frac{\Delta H_{\mathrm{p}}}{RT} - \frac{\Delta S_{\mathrm{p}}}{R} \qquad \ldots(5)$$

Therein, ΔH_{p} and ΔS_{p} represent the enthalpy and entropy changes that occur during polymerization; R is the gas constant (R = 8.314 J·mol^{-1}·K^{-1}).

3. Results

3.1. Synthesis and characterization of CMs

In this study, CMs with four ring sizes (CM-2, -5, -10, and -20) were synthesized respectively by reacting native Hb with bi-functional maleimide PEG with the respective molecular weights of 2, 5, 10, and 20 kDa (**Figure 1A**). In the SEC profile, CM-2, -5, -10, and -20 were observed respectively as peaks at 11.61, 11.37, 10.94, and 10.32 min (**Figure 2A**). A larger CM showed a shorter retention time with a wider peak width because of the conjugation of the longer PEG chain. Apparent molecular weights of CM-2, -5, -10, and -20 estimated respectively from calibration curve using globular protein markers[21] are 38, 53, 94, and 217 kDa, which differ from actual molecular weights of 67, 70, 75, and 85 kDa. This result indicates that PEGylated Hb shows quite different morphology from native globular proteins in the aqueous solution. Dynamic light scattering (DLS) measurements of CMs showed an increase in particle size and wide dispersion with the molecular weight of PEG moiety (**Table 1**), which supports the result obtained from SEC measurement.

The components of CM were clarified using SDS-PAGE analysis (**Figure 2B**). The band of free α subunits remained in all CMs. By contrast, the band of free β subunits disappeared completely; the bands *a*, *b*, *c*, and *d* of each component of two β subunits linked with PEG (β−PEG−β) appeared. In contrast to the SEC results, each β−PEG−β subunit showed reasonable molecular weights compared to those of marker proteins. These results indicate the cyclic structure of each monomer, and show site-specific conjugation between mal_2-PEG and two β subunits (Cys-93(β)) of an Hb molecule.[36]

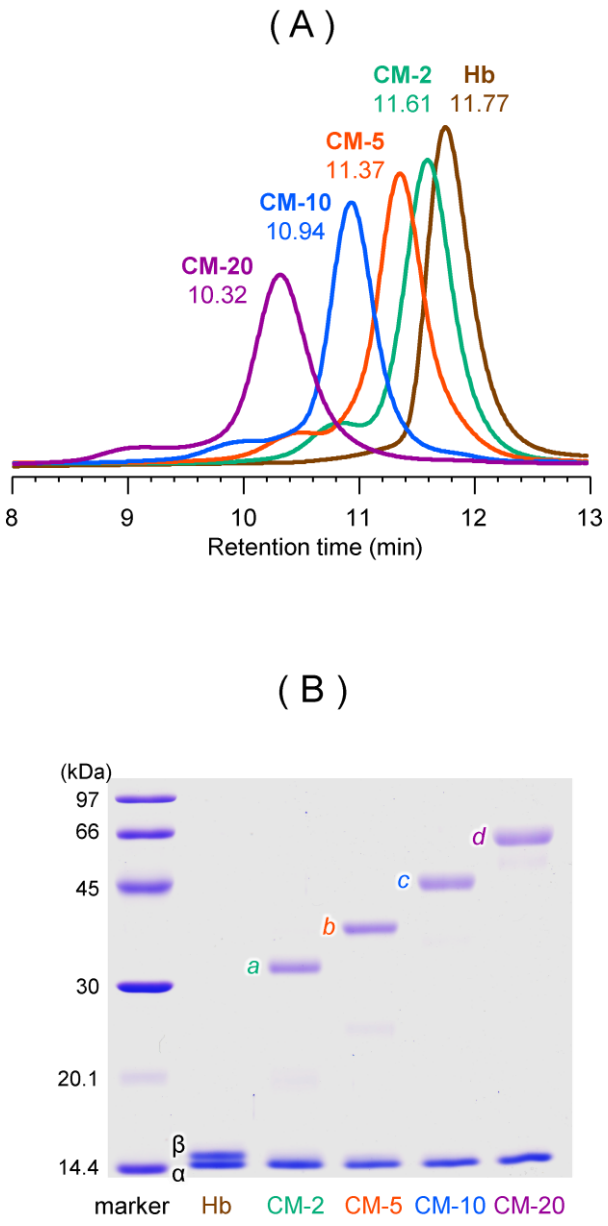

Figure 2. (A) SEC profiles of CM-2, -5, 10, -20, and native Hb. A larger CM showed a shorter retention time. (B) SDS-PAGE analysis of CM-2, -5, 10, -20, and native Hb. One Hb molecule consists of two α (15.1 kDa) and two β (15.8 kDa) subunits, whereas one CM molecule consists of two α subunits and one β−PEG−β subunit (bands *a*, *b*, *c*, and *d*: 33, 36, 42, and 52 kDa (calc.)).

Table 1. Summary of dynamic light scattering (DLS) measurements of native Hb and CMs

Sample	M_n of PEG moiety (kDa)	Particle diameter (avg. ± S.D., nm)
native Hb	—	7.7 ± 1.7[a]
CM-2	2.0	10.2 ± 1.6
CM-5	4.4	14.5 ± 3.9
CM-10	10.5	16.9 ± 6.1
CM-20	20.8	22.2 ± 10.8

a: data referred from ref. 21

3.2. Effects of CM ring size on COP measurements

The colloid osmotic pressure (COP, π) of each CM solution increases with the concentration of Hb units, *C*, similarly to native Hb (**Figure 3A**). In fact, CM containing the larger molecular weight PEG showed a steep increase in the π value as a function of *C*. For larger CM-5, -10, and -20, the plots of π/C versus *C* clearly showed quadratic curves, indicating that the third virial coefficients are not negligible because of the presence of S-ROP equilibrium, depending on *C* values (**Figure 3B**). The quadratic curve fittings of the plots of CMs based on **Eq. 2** are presented in **Table 2**. The plot of CM-2 is apparently closer to a linear relation than the larger CMs. However, we considered that quadratic curve fitting is appropriate also for CM-2 because the correlation coefficient (r^2) became smaller in the case of linear curve fitting (r^2 = 0.9825). The number average molecular weights (M_n) of CM-2, -5, -10, and -20 obtained from the intercept of the quadratic curve fitting are, respectively, 81, 88, 104, and 157 kDa. The M_n obtained from COP measurements are regarded as reflecting the molecular sizes of CMs in an infinitely diluted condition. The apparent M_n are much higher than the actual M_n (67, 70, 75, and

85 kDa) because of the large hydrodynamic volume of the PEG moieties.[37] To estimate the supramolecular interaction effects, COP of the fixed CM-10 (XLCM-10) in a ring-closed state by ββ-cross-linking was also measured (**Figure 3**, light blue). The COP of XLCM-10 was increased considerably, almost doubled, compared to that of CM-10.

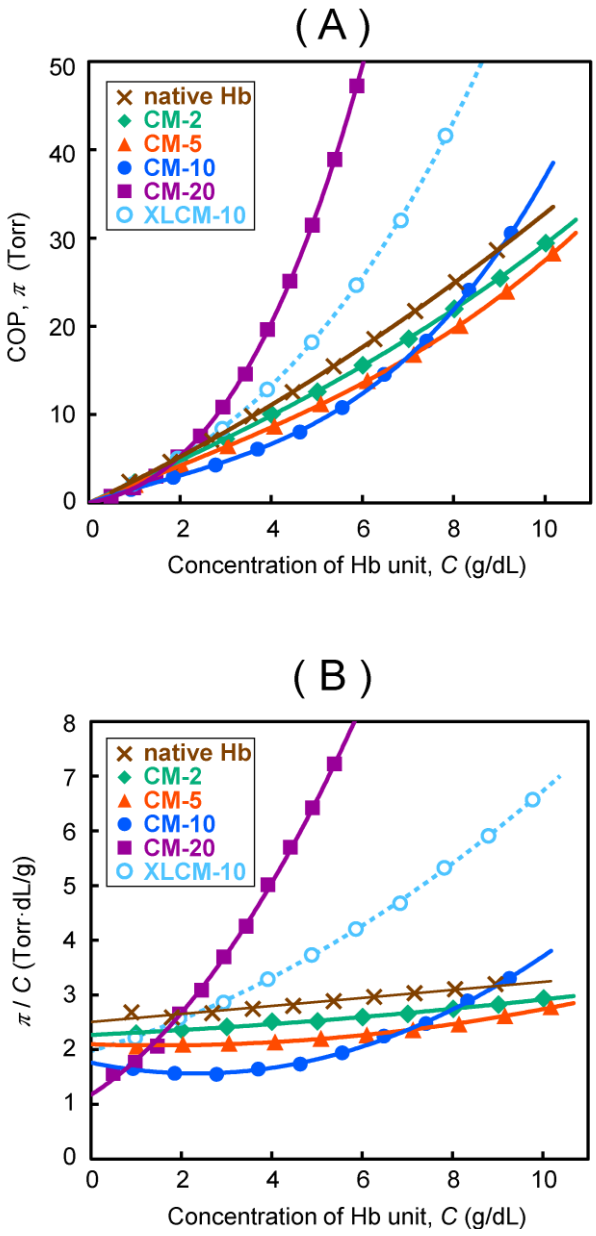

Figure 3. (A) Colloid osmotic pressure (COP, π) of native Hb (brown), CM-2 (green), CM-5 (orange), CM-10 (blue), CM-20 (purple), and XLCM-10 (light blue) as a function of the concentration of Hb units, *C*. (B) Plots showing π/C versus *C*. The plots of CMs and XLCM-10 show parabolic curves indicating that the third virial coefficients are not negligible. Data of native Hb and CM-10 were referred from a report of our earlier study.[21]

Table 2. Summary of quadratic curve fitting of π/C versus *C* plot in **Figure 3B** based on **Eq. 2**

Sample	Curve fitting based on **Eq. 2** $RT\,(1/M_n + A_2C + A_3C^2)$ (Torr·dL·g^{-1})	Correlation coefficient r^2	M_n ×10^{-3} (g·mol^{-1})	A_2 ×10^5 (mol·cm^3·g^{-2})	A_3 ×10^6 (mol·cm^6·g^{-3})
CM-2	2.270 + 0.039 *C* + 0.003 C^2	0.9916	81	2.1	1
CM-5	2.095 − 0.027 *C* + 0.009 C^2	0.9975	88	−1.5	5
CM-10	1.763 − 0.169 *C* + 0.036 C^2	0.9983	104	−9.2	20
CM-20	1.177 + 0.527 *C* + 0.110 C^2	0.9992	157	28.6	60
XLCM-10	1.977 + 0.242 *C* + 0.023 C^2	0.9997	93	13.1	13

Gas constant R = 62.364 Torr·L·mol^{-1}·K^{-1}, T = 294–297 K

3.3. Fixing the $\alpha_2\beta_2$ tetrameric structures of Hb unit of CMs in S-ROP equilibrium

CMs are converted reversibly to the corresponding supramolecular Hb polymers (SPs) through the S-ROP equilibrium. The progress of S-ROP is expected to depend critically on the initial monomer concentration $[M]_0$. All Hb units ($\alpha_2\beta_2$) in SPs and CMs were fixed by ββ-cross-linking using DBBF for evaluation of the S-ROP progress (**Figure 1B**). **Figure 4** presents SEC

profiles of the products after reacting DBBF with (**A**) CM-2, (**B**) CM-5, (**C**) CM-10, and (**D**) CM-20, at different $[M]_0$. When reacting CMs with DBBF at a lower $[M]_0$ of 0.050 mM (blue chromatograms), the CM structures were mainly fixed in an Hb unit to obtain the ββ-cross-linked cyclic Hb monomers: XLCMs. The peaks of XLCM-2, -5, -10, and -20 (11.58, 11.37, 10.94, and 10.30 min) showed almost equal retention times of the corresponding CMs (11.61, 11.37, 10.94, and 10.32 min), indicating that XLCMs have the same molecular size as those of CMs. In **Figure 4D**, peaks with shorter retention times of around 7.91 min were also observed. This result indicates the generation of a supramolecular assembly (SP-20) during the inter-molecular subunit exchange of αβ dimers between CM-20 molecules, even at a lower $[M]_0$ of 0.050 mM. To suppress this inter-monomer assembling, CM-20 was reacted with DBBF at more diluted $[M]_0$ of 0.010 mM (gray chromatogram in **Figure 4D**). The peaks around 7.91 min disappeared, indicating the selective fixing of the monomeric ring structure at this concentration.

The concentrations of CM-2, -5, -10, and -20 were adjusted to a higher $[M]_0$ of 1.00 mM for reaction with DBBF (green chromatograms in **Figures 4A–4D**). The relative peak intensities of XLCMs decreased in comparison with the case of ββ-cross-linking at 0.050 mM. Instead, the broad peaks of ββ-cross-linked supramolecular Hb polymers, XLSP-2, -5, -10, and -20, appeared respectively at approximately 10.81, 9.95, 6.41, and 6.40 min. The red chromatograms in **Figure 4A–4D** respectively show the ββ-cross-linked products of CM-2, -5, -10, and -20 at concentrated conditions of $[M]_0$ = 5.43, 3.10, 3.01, and 1.16 mM. The peak intensity of every remaining XLCM is markedly lower than that of ββ-cross-linked at a lower $[M]_0$. In **Figures 4A** and **4B**, XLSP-2 and -5 in red chromatograms were observed at 10.07 min and at 9.13 min as a left-shifted broad peak compared to those of green chromatograms. The result indicates the formation of oligomeric supramolecular assembly at a highly concentrated condition immediately before

reaction with DBBF. In **Figures 4C** and **4D**, XLSP-10 and -20 appear at ca. 6.30–6.40 min, which reaches to the fraction of void volume of the equipped column (protein KW-804). In the earlier report describing CM-10, polymer size comparable to the void volume is reportedly equivalent to that of a decamer or more.[21]

Each XLSP solution of the red chromatogram in **Figure 4** was diluted to [Hb] = 0.010 mM; the distribution of the particle diameter was obtained from DLS measurement (**Table 3**, Supporting Information **Figure S1**). The average particle diameters of XLSP-10 and -20 (exceeding 100 nm) were much larger than those of XLSP-2 (43.6 nm) and XLSP-5 (53.5 nm), respectively, which supports the SEC analysis (**Figure 4**). Actually, XLSP with an alternating structure of globules (XLHbs) and flexible chains (PEGs) is regarded as forming a random coil structure in an aqueous solution.

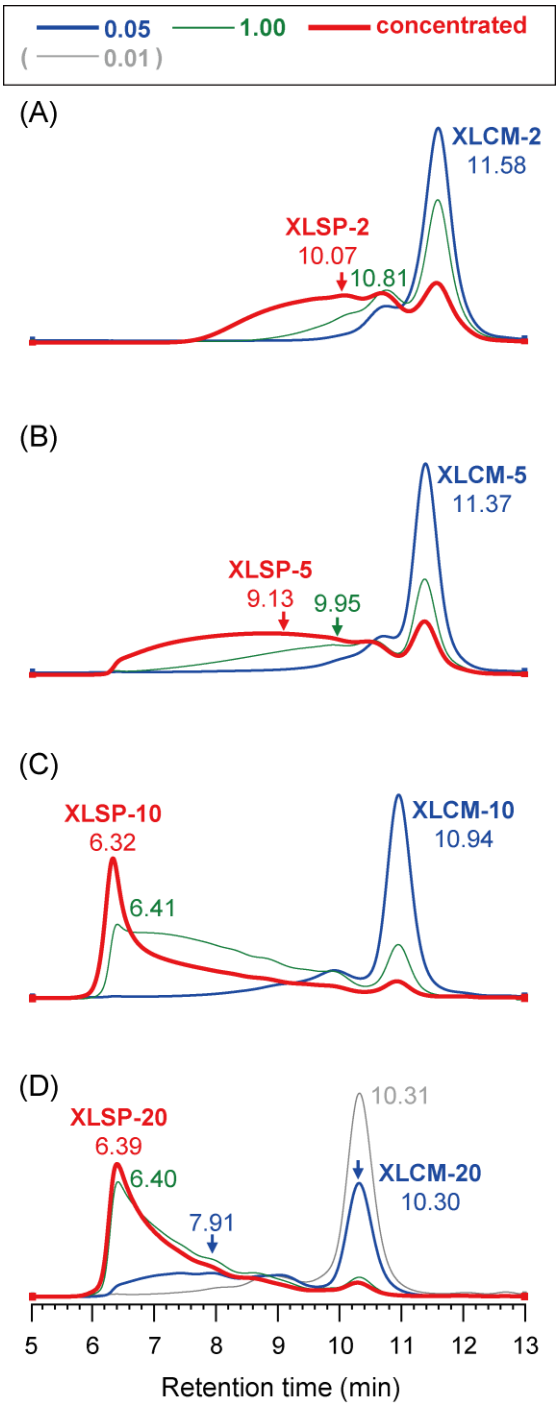

Figure 4. SEC profiles of the products after reacting DBBF with (A) CM-2, (B) CM-5, (C) CM-10, and (D) CM-20 at different $[M]_0$ of 0.050 mM (blue), 1.00 mM (green), concentrated conditions (5.43, 3.10, 3.01, and 1.16 mM for CM-2, -5, -10, and -20; red), and a highly diluted condition (0.010 mM, only for CM-20; gray).

Table 3. Summary of DLS measurements of XLSPs

Sample	$[M]_0$ at ββ-Cross-linking (mM)	Particle diameter (avg. ± S.D., nm)
XLSP-2	5.43	43.6 ± 22.6
XLSP-5	3.10	53.5 ± 30.2
XLSP-10	3.01	117.3 ± 64.2
XLSP-20	1.16	106.9 ± 61.3

The components of ββ-cross-linked products were analyzed using SDS-PAGE (**Figure 5**). Band *e* in Lane **A** for each CM coincided with β−PEG−β subunit (bands *a*, *b*, *c*, and *d* in **Figure 2B**). Band *e* disappeared by ββ-cross-linking at 0.050 mM. Alternatively, new band *f* with a lower mobility than band *e* appeared in each Lane **B**. Each band *f* was assigned as the PEGylated β−β component with a closed ring structure (β−β−ringPEG), which is one component of each XLCM. Both β−PEG−β and β−β−ringPEG are expected to have equal molecular weight. Actually, in the case of using 2 kDa PEG, bands *e* and *f* are located in an almost identical mobility. However, the difference in mobility between bands *e* and *f* increased with the molecular weight of PEG. The result indicates that conjugating PEG moiety has a larger hydrodynamic volume than the free chain when fixed in a ring structure. In CM-20 Lane **B**, a band *g* assigned as the polymeric β component was observed along with band *f*, which is consistent with the SEC result of partial polymerization (**Figure 4D**). This band *g* disappeared by reacting DBBF at a lower CM-20 concentration of 0.010 mM (Supporting Information, **Figure S2**).

In each lane **C**, a polymeric β component (poly(β−β−PEG)) was observed as a band *g* by reacting CM with DBBF at a higher concentration. Every band *g* showed markedly lower mobility in polyacrylamide gel, reflecting its larger molecular size of poly(β−β−PEG) than that of the 97 kDa protein marker. Free α subunits remained at every concentration, indicating the selective cross-linking of β subunits by reaction with DBBF.[6]

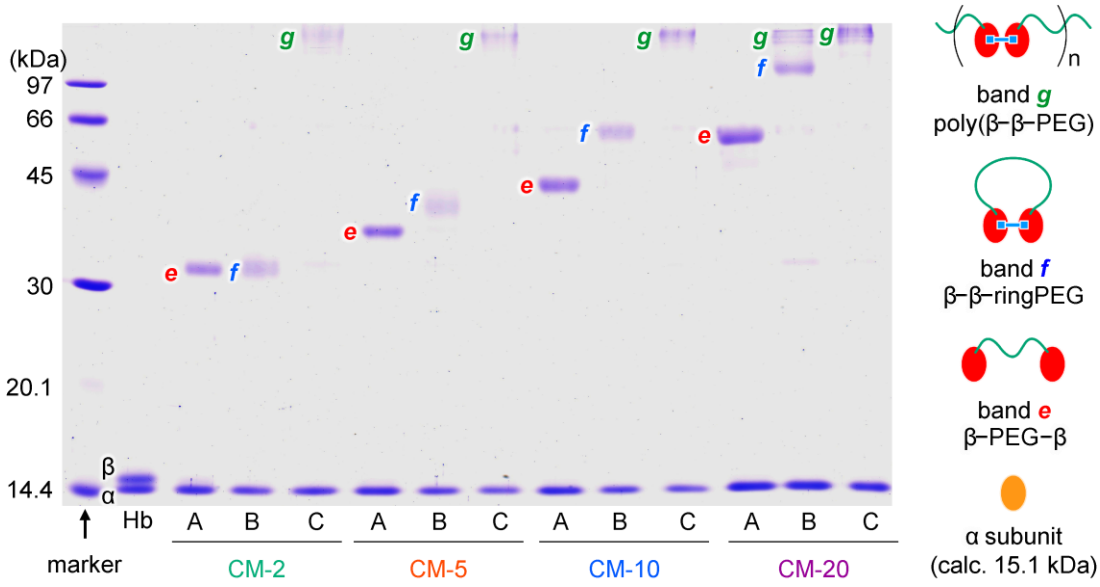

Figure 5. SDS-PAGE of CMs before and after ββ-cross-linking at different concentrations: Lanes **A**, CMs before adding DBBF; Lanes **B**, selectively synthesized XLCMs by reacting DBBF with CMs at a lower concentration of 0.050 mM; Lanes **C**, selectively synthesized XLSPs by reacting DBBF with CM-2, -5, -10, and -20 at higher concentrations of 5.43, 3.10, 3.01, and 1.16 mM, respectively. Bands *e* in Lanes **A** corresponding to β−PEG−β converted to bands *f* in Lanes **B** of the PEGylated β−β component with a closed ring structure (β−β−ringPEG) by ββ-cross-linking. In Lanes **C**, bands *g* of the polymeric component (poly(β−β−PEG)) were observed.

3.4. Quantification of supramolecular ring-chain equilibria

The CMs and SPs in the equilibrium state of S-ROP were ββ-cross-linked at several $[M]_0$. The relative ratios of XLCM (r_1) calculated using **Eq. 4** are shown for $[M]_0$ (**Figure 6**). The r_1 value decreased with $[M]_0$. A smaller CM showed a higher r_1 value when compared with the same $[M]_0$. The relative ratio of monomer and polymer after ββ-cross-linking is regarded as reflecting that immediately before adding DBBF.[21] Therefore, the r_1 value is regarded as representing the ratio of CM in the equilibrium state of S-ROP. The results suggest that the balance in **Scheme 1** tilts to the left (monomer-rich) at a lower $[M]_0$, while it tilts to the right (polymer-rich) at a higher $[M]_0$.

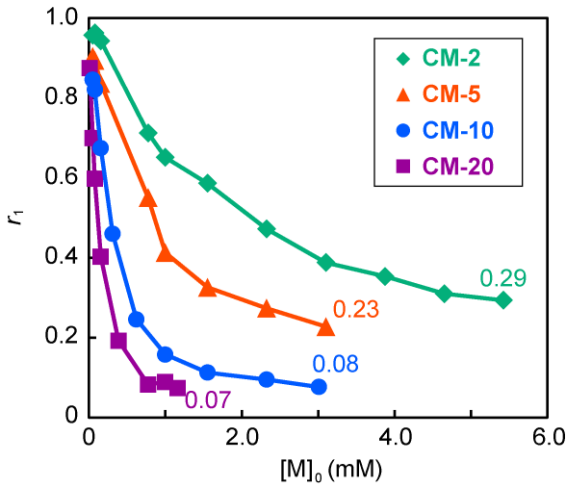

Figure 6. Relation between r_1 and $[M]_0$. The r_1 value is the relative ratio of XLCM obtained from **Eq. 4** based on the SEC analysis. $[M]_0$ is the initial monomer concentration for ββ-cross-linking. The r_1 values are regarded as reflecting the relative ratios of CM in the equilibrium state of S-ROP.

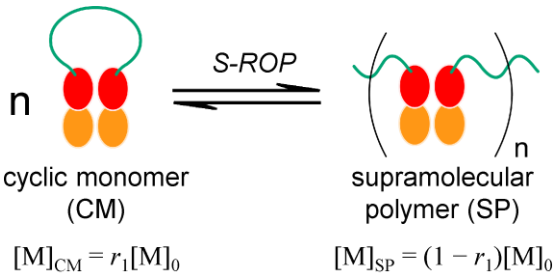

Scheme 1. S-ROP equilibrium of CM and SP immediately before ββ-cross-linking.

In the equilibrium state, the concentration of the remaining cyclic Hb monomer, described as $[M]_{CM}$, is obtained from the product of r_1 and $[M]_0$ (**Scheme 1**). The concentration of the monomer units constructing a supramolecular Hb polymer (SP), described as $[M]_{SP}$, is obtained from the product of $(1 - r_1)$ and $[M]_0$. The $[M]_{CM}$ and $[M]_{SP}$ of CM-2, -5, -10, and -20 calculated from **Figure 6** are shown for each $[M]_0$ (**Figure 7**). In all cases, $[M]_{CM}$ became a plateau, whereas $[M]_{SP}$ increased linearly at higher $[M]_0$. The critical monomer concentration $[M]_{crit}$, at which ring-opening polymerization initiates, is found from the intersection of the linear $[M]_{SP}$ line with the x-axis.[38] Results show that the $[M]_{crit}$ for CM-2, -5, -10, and -20 were, respectively, 0.856, 0.329, 0.125, and 0.063 mM. Ideally, $[M]_{crit}$ is expected to be equal to the asymptotic $[M]_{CM}$ at a higher $[M]_0$.[38,39] However, in practice, the slope of each $[M]_{SP}$ is less than 1; $[M]_{crit}$ is smaller than each asymptotic $[M]_{CM}$ (1.59, 0.70, 0.23, and 0.085 mM at the highest $[M]_0$).

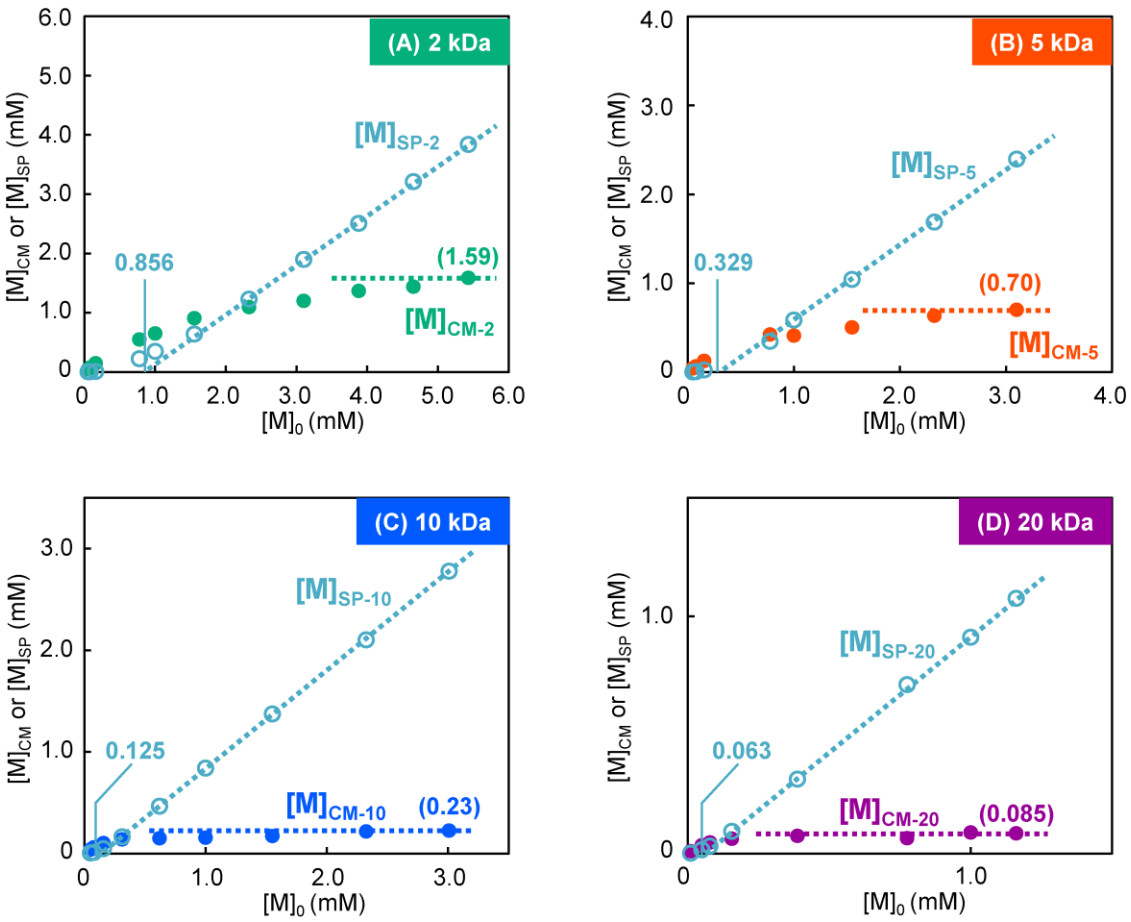

Figure 7. Plots of $[M]_{CM}$ and $[M]_{SP}$ of (A) CM-2, (B) CM-5, (C) CM-10, and (D) CM-20, at different $[M]_0$, where $[M]_{CM}$ and $[M]_{SP}$ are the concentrations of CM and SP in the equilibrium state of S-ROP (**Scheme 1**). $[M]_{SP}$ increased linearly with $[M]_0$, whereas $[M]_{CM}$ approached a constant value (as shown in parentheses, 1.59, 0.70, 0.23, and 0.085 mM at the highest $[M]_0$, respectively, for CM-2, -5, -10, and -20). The critical monomer concentrations $[M]_{crit}$ (0.856, 0.329, 0.125, and 0.063 mM) were obtained, respectively, from the intersection of linear $[M]_{SP}$ plots with x-axis for SP-2, -5, -10, and -20.[38]

3.5. Thermodynamic analysis of S-ROP equilibria

To evaluate the S-ROP thermodynamics of CMs, each 1.00 mM CM solution was reacted with DBBF at five temperatures: 4, 15, 25, 35, and 45 °C. The CM concentration in the equilibrium state ($[M]_{eq}$) was obtained as $[M]_{CM}$ at $[M]_0$ = 1.00 mM. The plots of $\ln[M]_{eq}$ for reciprocal T were almost horizontally flat in every CM (**Figure 8**). The result indicates that $[M]_{eq}$ is independent of the temperature in the region of 4−45 °C, and indicates that ΔH_p are negligibly small (**Table 4**). Actually, all the ΔH_p obtained from the slope are below 1 kJ·mol^{-1}. In contrast, ΔS_p obtained from the intercept increased with ring size of CMs from 26.8 to 33.2 kJ·mol^{-1}·K^{-1}. At 298 K, $T\Delta S_p$ is quite larger than ΔH_p for every CM, indicating the progress of entropy-driven S-ROP.

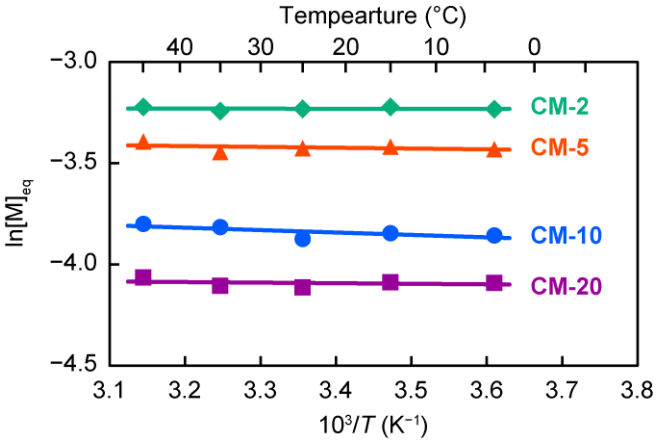

Figure 8. Relation between $\ln[M]_{eq}$ and reciprocal T. All reactions were conducted at $[M]_0$ of 1.00 mM. The $[M]_{eq}$ was obtained from the peak areas of ββ-cross-linked products in SEC analyses. The slopes, associated with polymerization enthalpy (ΔH_p), are almost zero. The polymerization entropy (ΔS_p) estimated from the intercept increases with the CM ring size.

Table 4. Thermodynamic parameters of S-ROP equilibria of 1.00 mM CMs obtained by linear fittings of plots in **Figure 8** based on the Dainton's equation (**Eq. 5**)

monomer	ΔH_p (kJ·mol^{-1})	ΔS_p (J·mol^{-1}·K^{-1})	$T\Delta S_p$ (kJ·mol^{-1}) [a]
CM-2	−0.01	26.8	7.99
CM-5	−0.33	27.3	8.14
CM-10	−1.00	28.5	8.50
CM-20	−0.23	33.2	9.90

a: at 298 K

4. Discussion

In this study, we clarified the thermodynamic mechanism of reversible supramolecular ring-opening polymerization (S-ROP) of cyclic Hb monomers (CMs). The produced supramolecular Hb polymers (SPs) and the remaining CMs in the equilibrium state were quantified as ββ-cross-linked products. Temperature dependencies of the equilibrium concentrations of CMs showed markedly positive entropy changes that increased with ring size. This report provides the first evidence elucidating the entropy-driven S-ROP for constructing protein-containing supramolecular polymers.

The CMs with four ring size (CM-2, -5, -10, and -20) were synthesized by reacting bi-functional maleimide PEGs (mal_2-PEG) with native Hb (**Figure 1A**). The CMs were characterized using SEC, DLS, COP, and SDS-PAGE (**Figures 2** and **3**, **Tables 1** and **2**). The yield of CM depends on the result of salting out fractionation for removing unreacted native Hb. In fact, CM-10 and CM-20 were easier to purify than either CM-2 or CM-5 because of the large difference in molecular weight compared to native Hb. The apparent molecular weights (M_n) of CM-2, -5, -10, and -20 estimated using COP analysis are, respectively, 81, 88, 104, and 157 kDa, which are larger from actual molecular weights of 67, 70, 75, and 85 kDa because of the conjugation of a flexible PEG chain with a large hydrodynamic volume.

It is noteworthy that the π/C versus C plots of all CMs in **Figure 3B** showed parabolic curves. Reportedly, the representative chemically modified Hbs, such as αα- and ββ-cross-linked, glutaraldehyde polymerized, *o*-raffinose polymerized, hydroxyethyl starch polymerized, and PEG coated Hbs, showed linear relations in π/C versus C plots similarly to unmodified Hb.[3,21,33] For these chemically modified Hbs, the third-order and the higher-order virial coefficients in **Eq. 2** are sufficiently negligible. Particularly, it is outstanding that the third virial coefficients A_3 are

not negligible for CMs (**Table 2**). Reportedly, A_3 reflects interaction among the three molecules.[40,41] The contribution of inter-molecular association by αβ dimers bound to PEG terminals is inferred to increase the third virial coefficient in COP measurement of CMs. Actually, a CM with a larger ring size showed larger A_3 because a larger CM was easier to polymerize. Such a considerably large A_3 indicates that CMs have inconsistent size at every concentration by the existence of a $[M]_0$ dependent S-ROP equilibrium. The timescale to reach the S-ROP equilibrated state is expected to be nearly instantaneous (in seconds) considering the dissociation rate constant (k_d = 2 s^{-1}) of $\alpha_2\beta_2$ tetramer to αβ dimers of native Hb.[42]

The inter-molecular association by αβ dimers described above can be suppressed by covalent fixation of the Hb unit ($\alpha_2\beta_2$). The XLCM-10, covalently fixed CM-10, showed almost double the COP of a non-fixed CM-10 (**Figure 3A**). This result indicates an almost half decrease in the number of particles compared with XLCM-10 by forming a supramolecular Hb polymer, SP-10, according to the inter-molecular association of CM-10 through S-ROP equilibrium. An intercept of the π/C plot of XLCM-10 in **Figure 3B** nearly coincided with that of CM-10, indicating a similar structure at a diluted concentration. The A_3 of XLCM-10 was lower than that of CM-10, which can be attributed to the suppression of interaction between αβ dimers (**Table 2**). However, the π/C plot of XLCM-10 still showed a quadratic curve despite the covalent fixation of an $\alpha_2\beta_2$ unit. Free PEG is known for its oncotic properties with showing of unambiguous A_3 in an aqueous solution by combination of osmolyte-solvent and osmolyte-osmolyte interactions.[43,44] The observed A_3 of XLCM-10 might be attributable to the contribution of such interactions of PEG moieties.

Our earlier report treating CM-10 showed that the cyclic Hb monomer induced S-ROP to construct a linear supramolecular Hb polymer.[21] The progress of S-ROP was confirmed by fixing

the Hb units ($\alpha_2\beta_2$) using a known site-specific ββ-cross-linking agent: DBBF. For this work, similarly, Hb units in CMs and in SPs are ββ-cross-linked to produce corresponding XLCMs and XLSPs (**Figures 4** and **5**). The XLCMs were obtained selectively at lower concentrations of 0.010−0.050 mM, whereas XLSPs were obtained dominantly at higher concentrations of 1.16−5.43 mM. The change in ββ-cross-linked product depends on the initial monomer concentration $[M]_0$, which indicates the reversible S-ROP equilibrium, as shown in **Scheme 1** immediately before adding DBBF. The relative ratio of remaining CM, r_1, eventually decreased concomitantly with increasing $[M]_0$ (**Figure 6**).

The concentration of the remaining CM ($[M]_{CM}$), obtained as $r_1[M]_0$, approached the constant value at a higher $[M]_0$ (**Figure 7**). Our earlier report described that asymptotic $[M]_{CM}$ for CM-10 was 0.176 mM.[21] The value almost coincides with the result presented herein (0.23 mM). The $[M]_{CM}$ values for CM-2 and -5 still increase with $[M]_0$, even at the highest 5.43 and 3.10 mM, which suggests that S-ROP has not progressed sufficiently. The critical monomer concentration $[M]_{crit}$, determined from intersection of linear $[M]_{SP}$ plot with the x-axis,[38] does not match the asymptotic $[M]_{CM}$ value because of such increase of $[M]_{CM}$. The decrease in $[M]_{crit}$ with an increase in the ring size of CM indicates that a larger CM is polymerized at a lower $[M]_0$ by facilitating S-ROP.

From studies of supramolecular polymer constructed via a metal–ligand coordination bond, the degree of polymerization (DP) depends critically upon the metal–ligand association constant, K_a, and the initial monomer concentration, $[M]_0$.[45] In the study, DP of metal–ligand coordination supramolecular polymer was estimated at $[M]_0 = 1$ mM. Supramolecular polymer with DP ≈ 10 can be formed when $K_a = 10^5$ M^{-1}; that with DP ≈ 100 can be formed when $K_a = 10^7$ M^{-1}.[45] For native Hb, the K_a of αβ dimers to $\alpha_2\beta_2$ tetramer is reportedly 10^5–10^6 M^{-1}.[23,46,47]

Judging from the K_a values, the non-covalent interaction between αβ dimers has potential for application to construct a supramolecular polymer with DP > 10 at $[M]_0$ > 1 mM. Actually, in the present SEC results of ββ-cross-linking at $[M]_0$ = 1.00 mM (green chromatograms in **Figure 4**), CM-20 was efficiently ring-opened (r_1 = 0.088) and polymerized to form XLSP-20 with a molecular size reaching to the column void volume (DP >10). However, CM-2 only slightly ring-opened (r_1 = 0.65) at $[M]_0$ = 1.00 mM; DP of the produced XLSP-2 was estimated as far smaller than ten. The result suggests interference of S-ROP of CM when using a short PEG linker. Acharya and co-workers earlier reported the synthesis and characterization of ββ-cross-linked Hb through 2 kDa PEG with structure similar to our CM-2.[31] No oligomer was reportedly observed in their study. They explained predictively that a thermodynamically stable cyclic structure was produced preferentially because the 2 kDa PEG length coincided with the intra-molecular distance between two Cys-93(β) of an $\alpha_2\beta_2$ molecule.

The proximity of two αβ dimers located at both ends of a PEG chain increases the local concentration of the αβ dimer, which facilitates ring-closure. Such an effect was proposed by Kuhn[48] as a concept of effective concentration of chain end groups.[38] For CMs, increasing the length of the PEG linker from 2 kDa is expected to decrease the effective concentration because two αβ dimers at the PEG ends become mutually distal. A rough approximation of the effective concentration equal to $[M]_{crit}$ showed that the intra-molecular distances (d) between PEG terminated αβ dimers for CM-2, -5, -10, and -20 are estimated respectively as 61, 84, 117, and 147 Å (Supporting Information). On the other hand, the root-mean-squared end-to-end distances (r_{rms}) of free random chains of 2, 5, 10, and 20 kDa PEGs can be estimated theoretically as 35, 51, 79, and 111 Å, respectively (Supporting Information).[49] Each d value was found to be fairly close to the corresponding r_{rms} value, but ca. 1.5 times larger. These estimation results suggest

that S-ROP initiates when the CM molecules approach each other within the linker length. The 1.5 times differences between d and r_{rms} is expected to be attributable to the excluded volume of an Hb molecule (ca. 50−60 Å diameter)[29], which is ignored in estimation of the d value.

In a general thermodynamic analysis based on Dainton's equation (**Eq. 5**)[35] for ROP equilibrium of low molecular weight cyclic monomers, represented by lactones, the effects of the number of ring members on polymerization enthalpy (ΔH_p) and entropy (ΔS_p) were well established.[34] Actually, ΔH_p reflects the loss of an internal strain energy of a cyclic monomer, and ΔS_p reflects the increase in randomness associated with ROP. A lactone with a smaller ring size (below the seven-membered ring such as ε-caprolactone (C_6)) shows considerably negative ΔH_p, indicating that enthalpy-driven ROP proceeds as a result of releasing the ring-strain. However, an ω-pentadecalactone (C_{15}) with a large number of ring members shows positive ΔS_p (23 $J \cdot mol^{-1} \cdot K^{-1}$) with negligibly small ΔH_p (3 $kJ \cdot mol^{-1}$).[34,50] Therefore, the ROP mechanism is entropy-driven.

For the present case of S-ROP of CMs, similarly to the case of ω-pentadecalactone, CMs showed a markedly positive ΔS_p which increased with ring size (26.8−33.2 $J \cdot mol^{-1} \cdot K^{-1}$, **Table 4**). Actually, $[M]_{eq}$ was temperature-independent at 4−45 °C, at which Hb does not denature (**Figure 8**); ΔH_p was negligibly small ($\leq$ 1 $kJ \cdot mol^{-1}$) for every CM. These results demonstrate the entropy-driven mechanism of S-ROP for all CMs and the absence of ring strain, even in the smallest CM-2. The same analytical method was applied to enthalpy-driven S-ROP of low molecular weight monomers using metal–ligand coordination bonds.[51] However, no reports of the relevant literature has described a demonstration of the mechanism of entropy-driven S-ROP for giant monomers containing protein. Our findings are expected to provide important insights for researchers investigating other supramolecular protein polymers.

S-ROP has several advantages as a method for synthesizing HBOCs. The regularly alternating Hb−PEG sequence enables precise control of polymer geometry. Moreover, it has potential for achieving a higher DP as compared to the conventional Hb polymers. For conventional glutaraldehyde-polymerized Hbs (poly-Hbs), which had been clinically tested HBOCs from the late 1990s to the early 2000s,[11] minor components with low DP caused cardiovascular adverse effects.[12] Reportedly, such poly-Hbs had an average DP below five.[10] Our strategy using S-ROP realizes polymerized Hbs with notably larger particle diameters exceeding 100 nm for XLSP-10 and XLSP-20 (**Table 3**). Results of our present study of fundamental thermodynamic mechanism of S-ROP are expected to guide the future design of structurally regulated and highly polymerized Hb architectures.

For HBOCs, which contain Hb polymers, a larger particle size is desirable for preventing extravasation that causes vasoconstriction.[52] For this reason, many of current generation HBOCs tend to have micrometer or submicrometer dimensions.[3,4,14−16, 52−56] From our viewpoint of improving the DP, a larger CM is desirable. A larger molecular weight of the linker is associated with higher DP and lower $[M]_{crit}$. However, a limit to solubility exists for each CM because of the giant molecular masses of Hb molecules and PEG linkers. Actually, DP is estimated roughly as $[M]_0/[M]_{eq}$ at each concentration.[21] Based on estimation of the empirical decreases of maximal $[M]_0$ and $[M]_{eq}$ according to the increase of PEG molecular weight, CM using a PEG linker of about 37 kDa is estimated as reaching the highest DP (Supporting Information, **Figure S6**).

Of course, DP is just one of the factors related to the function of HBOCs. Scalability is an important consideration in the future implications of S-ROP. In the current stage, the salting out fractionation process lowers the synthetic yield of CM. Once this difficulty is resolved, scaling

up will be achieved easily because no particularly complicated reaction or instrument is necessary for synthesizing XLSPs. We reported earlier that XLSP-10 showed higher oxygen affinity (P_{50} = 5.2 Torr) and lower cooperativity (Hill number, n = 1.1) than native Hb (P_{50} = 8.2 Torr, n = 2.2) because of PEGylation at Cys-93(β) and ββ-cross-linking at Lys-82(β).[21] Physicochemical characteristics such as Hb concentration, oxygen affinity, COP, viscosity, stability to oxidation, and free Hb content must be considered comprehensively for optimizing the structure of HBOCs for efficient oxygen transport with reduced toxicity.

5. Conclusion

Our present work evaluated the entropy-driven mechanism of supramolecular ring-opening polymerization (S-ROP) of cyclic Hb monomers (CMs) for constructing Hb−PEG alternating polymers. We examined S-ROP for four CMs with different ring sizes. The largest CM using a 20 kDa PEG linker (CM-20) achieved the highest polymerization yield because of its lowest critical monomer concentration, $[M]_{crit}$. Thermodynamic analysis of S-ROP clearly demonstrated its entropy-driven mechanism. Using this technique based on supramolecular polymerization, not only a linear Hb−PEG alternating polymer but also a three-dimensional Hb architecture of structural regularity will be produced as next-generation HBOCs in the near future.

Supporting Information

Supporting Information includes detailed information related to DLS measurements of CMs and SPs, SDS-PAGE characterization of XLCM-20, estimation of intra-molecular distance

between αβ dimers, estimation of root-mean-squared end-to-end distance of free PEG chain, and empirical PEG molecular weight dependence of maximal $[M]_0$, $[M]_{eq}$, and DP.

Acknowledgments

This research was supported by a Grant-in-Aid for Scientific Research (Kiban C, No. 17K01367) from the Japan Society for the Promotion of Sciences (JSPS).

Author Information

Corresponding Author

*E-mail: hirosakai@naramed-u.ac.jp

ORCID

Takashi Matsuhira: 0000-0003-2429-9847

Hiromi Sakai: 0000-0002-0681-3032

Author Contributions

T.M. and H.S. conceived the study and designed the experiments. T.M. conducted experiments and data analyses. T.M. and H.S. wrote the manuscript. All authors have given their approval to the final version of the manuscript.

Notes

The authors declare that none has any competing financial interest.

References

(1) Chang, T. M. S. Therapeutic applications of polymeric artificial cells. *Nat. Rev. Drug Discov.* **2005**, *4*, 221–235.

(2) Savitsky, J. P.; Doczi, J.; Black, J.; Arnold, J. D. A clinical safety trial of stroma-free hemoglobin. *Clin. Pharmacol. Ther.* **1978**, *23*, 73−80.

(3) Sakai, H.; Yuasa, M.; Onuma, H.; Takeoka, S.; Tsuchida, E. Synthesis and physicochemical characterization of a series of hemoglobin-based oxygen carriers: objective comparison between cellular and acellular types. *Bioconjugate Chem.* **2000**, *11*(1), 56−64.

(4) Sakai, H.; Sou, K.; Tsuchida, E. Hemoglobin-vesicles as an artificial oxygen carrier. *Methods Enzymol.* **2009**, *465*, 363–384.

(5) Chatterjee, R.; Welty, E. V.; Walder, R. Y.; Pruitt, S. L.; Rogers, P. H.; Arnone, A.; Walder, J. A. Isolation and characterization of a new hemoglobin derivative cross-linked between the α chains (Lysine 99α_1 → Lysine 99α_2). *J. Biol. Chem.* **1986**, *261*(21), 9929−9937.

(6) Matsuhira, T.; Kure, T.; Yamamoto, K.; Sakai, H. Analysis of dimeric αβ subunit exchange between PEGylated and native hemoglobins ($\alpha_2\beta_2$ tetramer) in an equilibrated state by intramolecular ββ-crosslinking. *Biomacromolecules* **2018**, *19*(8), 3412−3420.

(7) Manjula, B. N.; Tsai, A. G.; Intaglietta, M.; Tsai, C. H.; Ho, C.; Smith, P. K.; Perumalsamy, K.; Kanika, N. D.; Friedman, J. M.; Acharya, S. A. Conjugation of multiple copies of polyethylene glycol to hemoglobin facilitated through thiolation: influence on hemoglobin structure and function. *Protein J.* **2005**, *24*(3), 133–146.

(8) Misra, H.; Lickliter, J.; Kazo, F.; Abuchowski, A. PEGylated carboxyhemoglobin bovine (SANGUINATE): results of a phase I clinical trial. *Artif. Organs* **2014**, *38*, 702−707.

(9) Tomita, D.; Kimura, T.; Hosaka, H.; Daijima, Y.; Haruki, R.; Ludwig, K.; Böttcher, C.; Komatsu, T. Covalent core-shell architecture of hemoglobin and human serum albumin as an artificial O_2 carrier. *Biomacromolecules* **2013**, *14*(6), 1816–1825.

(10) Day, T. K. Current development and use of hemoglobin-based oxygen-carrying (HBOC) solutions. *J. Vet. Emerg. Crit. Care* **2003**, *13*, 77−93.

(11) Modery-Pawlowski, C. L.; Tian, L. L.; Pan, V.; Sen Gupta, A. Synthetic approaches to RBC mimicry and oxygen carrier systems. *Biomacromolecules* **2013**, *14*(4), 939–948.

(12) Williams A.T.; Muller, C. R.; Eaker, A. M.; Belcher, D. A.; Bolden-Rush, C.; Palmer, A. F.; Cabrales, P. Polymerized hemoglobin with increased molecular size reduces toxicity in healthy guinea pigs. *ACS Appl. Bio Mater.* **2020**, *3*(5), 2976–2985.

(13) Yu, B. L.; Shahid, M.; Egorina, E. M.; Sovershaev, M. A.; Raher, M. J.; Lei, C.; Wu, M. X.; Bloch, K. D.; Zapol, W. M. Endothelial dysfunction enhances vasoconstriction due to scavenging of nitric oxide by a hemoglobin-based oxygen carrier. *Anesthesiology* **2010**, *112*, 586−594.

(14) Xiong, Y.; Steffen, A.; Andreas, K.; Müller, S.; Sternberg, N.; Georgieva, R.; Bäumler, H. Hemoglobin-based oxygen carrier microparticles: synthesis, properties, and *in vitro* and *in vivo* investigations. *Biomacromolecules* **2012**, *13*(10), 3292–3300.

(15) Ohta, S.; Hashimoto, K.; Fu, X.; Kamihira, M.; Sakai, Y.; Ito, T. Development of human-derived hemoglobin-albumin microspheres as oxygen carriers using Shirasu porous glass membrane emulsification. *J. Biosci. Bioeng.* **2018**, *126*(4), 533–539.

(16) Hickey, R.; Palmer, A. F. Synthesis of hemoglobin-based oxygen carrier nanoparticles by desolvation precipitation. *Langmuir* **2020**, *36*(47), 14166–14172.

(17) Yan, W.; Shen, L.; Yu, W.; Wang, Y.; Wang, Q.; You, G.; Zhao, L.; Zhou, H.; Hu, T. A triply modified human adult hemoglobin with low oxygen affinity, rapid autoxidation and high tetramer stability. *Int. J. Biol. Macromol.* **2020**, *159*, 236−242.

(18) Boykins, R. A.; Buehler, P. W.; Jia, Y.; Venable, R.; Alayash, A. I. *O*-raffinose crosslinked hemoglobin lacks site-specific chemistry in the central cavity: structural and functional consequences of β93Cys modification. *Proteins* **2005**, *59*, 840–855.

(19) Kluger, R.; Zhang, J. Hemoglobin dendrimers: functional protein clusters. *J. Am. Chem. Soc.* **2003**, *125*(20), 6070−6071.

(20) Wollocko, H.; Wollocko, B. M.; Wollocko, J.; Grzegorzewski, W.; Smyk, L. OxyVita®C, a next-generation haemoglobin-based oxygen carrier, with coagulation capacity (OVCCC). Modified lyophilization/spray-drying process: proteins protection. *Artif. Cells Nanomed. Biotechnol.* **2017**, *45*, 1350−1355.

(21) Matsuhira, T.; Yamamoto, K.; Sakai, H. Ring-opening polymerization of hemoglobin. *Biomacromolecules* **2019**, *20*(4), 1592−1602.

(22) Lehn. J. M. Perspectives in supramolecular chemistry – from molecular recognition towards molecular information processing and self-organization. *Angew. Chem. Int. Ed.* **1990**, *27*(1), 89–112.

(23) Hu, T.; Li, D.; Wang, J.; Wang, Q.; Liang, Y.; Su, Y.; Ma, G.; Su, Z.; Wang, S. Propylbenzmethylation at Val-1(α) markedly increases the tetramer stability of the PEGylated hemoglobin: a comparison with propylation at Val-1(α). *Biochim. Biophys. Acta* **2012**, *1820*(12): 2044–2051.

(24) Oohora, K.; Kajihara, R.; Fujimaki, N.; Uchihashi, T.; Hayashi, T. A ring-shaped hemoprotein trimer thermodynamically controlled by the supramolecular heme-heme pocket interaction. *Chem. Commun.* **2019**, *55*(11), 1544–1547.

(25) Staples, J. K.; Oshabena, K. M.; Horne, W. S. A modular synthetic platform for the construction of protein-based supramolecular polymers via coiled-coil self-assembly. *Chem. Sci.* **2012**, *3*, 3387–3392.

(26) Kobayashi, N.; Inano, K.; Sasahara, K.; Sato, T.; Miyazawa, K.; Fukuma, T.; Hecht, M. H.; Song, C.; Murata, K.; Arai, R. Self-assembling supramolecular nanostructures constructed from de novo extender protein nanobuilding blocks. *ACS Synth. Biol.* **2018**, *7*(5), 1381–1394.

(27) Bilgiçer, B.; Thomas, S. W. third; Shaw, B. F.; Kaufman, G. K.; Krishnamurthy, V. M.; Estroff, L. A.; Yang, J.; Whitesides, G. M. A non-chromatographic method for the purification of a bivalently active monoclonal IgG antibody from biological fluids. *J. Am. Chem. Soc.* **2009**, *131*(26), 9361–9367.

(28) Bastings, M. M. C.; De Greef, T. F. A.; Van Dongen, J. L. J.; Merkx, M.; Meijer, E. W. Macrocyclization of enzyme-based supramolecular polymers. *Chem. Sci.* **2010**, *1*, 79–88.

(29) Fernandez, E. J.; Abad-Zapatero, C.; Olsen, K. W. Crystal structure of Lysβ(1)82-Lysβ(2)82 crosslinked hemoglobin: a possible allosteric intermediate. *J. Mol. Biol.* **2000**, *296*(5), 1245–1256.

(30) Martello, M. T.; Burns, A.; Hillmyer, M. Bulk ring-opening transesterification polymerization of the renewable δ-decalactone using an organocatalyst. *ACS Macro Lett.* **2012**, *1*(1), 131–135.

(31) Manjula, B. N.; Malavalli, A.; Smith, P. K.; Chan, N. L.; Arnone, A.; Friedman, J. M.; Acharya, S. A. Cys-93-ββ-succinimidophenyl polyethylene glycol 2000 hemoglobin A. Intramolecular cross-bridging of hemoglobin outside the central cavity. *J. Biol. Chem.* **2000**, *275*(8), 5527–5534.

(32) Matsuhira, T; Osaki, S. Molecular weight of *Nephila clavata* spider silk. *Polym. J.* **2015**, *47*, 456–459.

(33) Vandegriff, K. D.; McCarthy, M.; Rohlfs, R. J.; Winslow, R. M. Colloid osmotic properties of modified hemoglobins: chemically cross-linked versus polyethylene glycol surface-conjugated. *Biophys. Chem.* **1997**, *69*(1), 23−30.

(34) Duda, A.; Kawalski, A. *Chapter 1*, in *Handbook of Ring-Opening Polymerization*; Dubois, P.; Coulembier, O.; Raquez, J. M. Eds.; Wiley-VCH: **2009**; pp 1–52.

(35) Dainton, F. S.; Ivin, K. J. Some thermodynamic and kinetic aspects of addition polymerization. *Q. Rev. Chem. Soc.* **1958**, *12*, 61–92.

(36) Manjula, B. N.; Tsai, A.; Upadhya, R.; Perumalsamy, K.; Smith, P. K.; Malavalli, A.; Vandegriff, K.; Winslow, R. M.; Intaglietta, M.; Prabhakaran, M.; Friedman, J. M.; Acharya, S. A. Site-specific PEGylation of hemoglobin at Cys-93(β): correlation between the colligative properties of the PEGylated protein and the length of the conjugated PEG chain. *Bioconjugate Chem.* **2003**, *14*(2), 464–472.

(37) Li, D.; Manjula, B. N.; Acharya, S. A. Extension arm facilitated PEGylation of hemoglobin: correlation of the properties with the extent of PEGylation. *Protein J.* **2006**, *25*, 263–274.

(38) De Greef, T. F.; Smulders, M. M.; Wolffs, M.; Schenning, A. P.; Sijbesma, R. P.; Meijer, E. W. Supramolecular polymerization. *Chem. Rev.* **2009**, *109*(11), 5687–5754.

(39) Xiao, T.; Zhong, W.; Qi, L.; Gu, J.; Feng, X.; Yin, Y.; Li. Z. Y.; Sun, X. Q.; Cheng, M.; Wang, L. Ring-opening supramolecular polymerization controlled by orthogonal non-covalent interactions. *Polym. Chem.* **2019**, *10*(24), 3342−3350.

(40) Nishi, Y.; Nakamura, Y.; Norisue, T. Effects of chain ends and three-segment interactions on second and third virial coefficients of four-arm star polystyrenes. *Polym. J.* **2009**, *41*, 58−62.

(41) Yamakawa, H.; Abe, F.; Einaga, Y. Effects of chain ends on the third virial coefficient for polymer chains. Oligo- and polystyrenes and oligo- and poly(methyl methacrylate)s. *Macromolecules* **1994**, *27*(12), 3272–3275.

(42) Nagel, R. L.; Gibson, Q. H. The binding of hemoglobin to haptoglobin and its relation to subunit dissociation of hemoglobin. *J. Biol. Chem.* **1971**, *246*(1), 69–73.

(43) Hasse, H.; Kany, H.-P.; Tintinger, R.; Maurer, G. Osmotic virial coefficients of aqueous poly(ethylene glycol) from laser-light scattering and isopiestic measurements. *Macromolecules* **1995**, *28*(10), 3540–3552.

(44) Cohen, J. A.; Highsmith, S. An improved fit to Website osmotic pressure data. *Biophys J.* **1997**, *73*(3), 1689–1694.

(45) Yang, L.; Tan, X.; Wang, Z.; Zhang, X. Supramolecular polymers: Historical development, preparation, characterization, and functions. *Chem. Rev.* **2015**, *115*(15), 7196−7239.

(46) Valdes, R. Jr. Modification of human haemoglobin with glucose 6-phosphate enhances tetramer–dimer subunit dissociation. *Biochem. J.* **1986**, *239*(3), 769–772.

(47) Arisaka, F.; Nagai, Y.; Nagai, M. Dimer-tetramer association equilibria of human adult hemoglobin and its mutants as observed by analytical ultracentrifugation. *Methods* **2011**, *54*(1), 175–180.

(48) Kuhn, W. Über die gestalt fadenförmiger moleküle in lösungen. *Kolloidn. Zh.* **1934**, *68*, 2–15.

(49) Powers, S.P.; Foo, I.; Pinon, D.; Klueppelberg, U. G.; Hedstrom, J. F.; Miller, L. J. Use of photoaffinity probes containing poly(ethylene glycol) spacers for topographical mapping of the cholecystokinin receptor complex. *Biochemistry* **1991**, *30*(3), 676–682.

(50) Yevstropov, A. A.; Lebedev, B. V.; Kipatisova, Ye. G. Thermodynamics of pentadecanolactone, of the process of its polymerization and of the resultant polypentadecanolactone in the 0–400 K region. *Polymer Science U.S.S.R.* **1983**, *25*(8), 1951–1960.

(51) Musgrave, R. A.; Russell A. D.; Hayward, D. W.; Whittell, G. R.; Lawrence, P. G.; Gates, P. J.; Green, J. C.; Manners, I. Main-chain metallopolymers at the static–dynamic boundary based on nickelocene. *Nature Chem.* **2017**, *9*, 743–750.

(52) Sakai, H.; Hara, H.; Yuasa, M.; Tsai, A. G.; Takeoka, S.; Tsuchida, E.; Intaglietta, M. Molecular dimensions of Hb-based O_2 carriers determine constriction of resistance arteries and hypertension. *Am. J. Physiol. Heart Circ. Physiol.* **2000**, *279*, H908–915.

(53) Sakai, H.; Sato, A.; Takeoka, S.; Tsuchida, E. Mechanism of flocculate formation of highly concentrated phospholipid vesicles suspended in a series of water-soluble biopolymers. *Biomacromolecules* **2009**, *10*, 2344–2350.

(54) Kettisen, K.; Bülow, L; Sakai, H. Potential electron mediators to extract electron energies of RBC glycolysis for prolonged in vivo functional lifetime of hemoglobin vesicles. *Bioconjugate Chem.* **2015**, *26*(4), 746–754.

(55) Gao, W.; Bian, Y.; Chang, T. M. S. Novel nanodimension artificial red blood cells that act as O_2 and CO_2 carrier with enhanced antioxidant activity: PLA-PEG nanoencapsulated polySFHb-superoxide dismutase-catalase-carbonic anhydrase. *Artif. Cells Nanomed. Biotechnol.* **2013**, *41*(4), 232–239.

(56) Arifin, D. R.; Palmer, A. F. Polymersome encapsulated hemoglobin: a novel type of oxygen carrier. *Biomacromolecules* **2005**, *6*(4), 2172–2181.

Table of Contents Graphic

This page is for Table of Contents Use Only.

Manuscript title: Entropy-Driven Supramolecular Ring-Opening Polymerization of Cyclic Hemoglobin Monomer for Constructing Hemoglobin−PEG Alternating Polymer with Structural Regularity

Authors: Takashi Matsuhira, Hiromi Sakai

Table of contents graphic (TOC):